

# Quantum spin pumping with adiabatically modulated magnetic barrier's

Ronald Benjamin\* and Colin Benjamin†

*Institute of Physics, Sachivalaya Marg, Bhubaneswar 751 005, Orissa, India*

A quantum pump device involving magnetic barriers produced by the deposition of ferro magnetic stripes on hetero-structures is investigated. The device for dc- transport does not provide spin-polarized currents, but in the adiabatic regime, when one modulates two independent parameters of this device, spin-up and spin-down electrons are driven in opposite directions, with the net result being that a finite net spin current is transported with negligible charge current. We also analyze our proposed device for inelastic-scattering and spin-orbit scattering. Strong spin-orbit scattering and more so inelastic scattering have a somewhat detrimental effect on spin/charge ratio especially in the strong pumping regime. Further we show our pump to be almost noiseless, implying an optimal quantum spin pump.

PACS numbers: 73.23.Ra, 05.60.Gg, 72.10.Bg

## I. INTRODUCTION

Present day improvements in technology are governed by two major constraints speed and size. Circuit components are slowly shrinking while their speed continues to increase. However there is limit to miniaturization. Making smaller components is not only costly but also the procedure inherently difficult. Further future miniature devices are proposed to be built at mesoscopic lengths where unlike recent times, quantum interference effects will play a major role. A peculiar and exciting mesoscopic device is the quantum pump<sup>1,2,3</sup> which has been shown to be adept at implementing rectification<sup>4</sup> and spin-polarization<sup>5,6</sup>. Recently a spin-polarized pump<sup>7</sup> has also been experimentally realized based on the theoretical formulations of Ref. 8. Among the many mesoscopic devices proposed, those which are effective in providing spin polarized transport are the most prized, as these are much more resilient to the vagaries of dephasing. In this work we propose a quantum spin pump, aided by the adiabatic modulation of magnetic barriers. A single magnetic barrier does not provide for spin polarized transport, but supplemented by adiabatic modulations we can convert it to a cent percent polarizer.

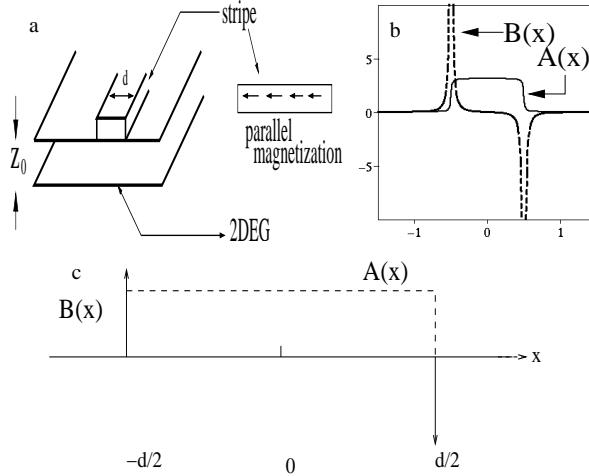


FIG. 1: (a) The device- On top of a 2DEG a parallelly magnetized magnetic stripe is placed. (b) The realistic magnetic field profile in a 2DEG along-with the magnetic vector potential for the device represented in (a). (c) The model magnetic field (delta function  $B(x)$ ) profile along with the magnetic vector potential  $A(x)$ .

## II. MODEL

In this work we propose a spin polarizer based on quantum pumping. The model of our proposed device is exhibited in Fig. 1. It is essentially a 2DEG in the  $xy$  plane with a magnetic field in the  $z$ -direction. The magnetic field profile

we consider is of delta function type for simplicity,  $\mathbf{B} = B_z(x)\hat{z}$  with  $B_z(x) = B_0[\delta(x+d/2) - \delta(x-d/2)]$ , wherein  $B_0$  gives the strength of the magnetic field and  $d$  is the separation between the two  $\delta$  functions (see Fig.1(c)). The above form of the magnetic field is an approximation of the more general form seen when parallelly magnetized ferromagnetic materials are lithographically patterned on a 2DEG (Fig.1(b)). Magnetic barrier's can not only be formed by this method but also when a conduction stripe with current driven through it is deposited on a 2DEG, and also when a super-conductor plate is deposited on a 2DEG, see Refs.[9,10] for details.

A 2DEG in the  $xy$  plane with a magnetic field pointing in the  $z$  direction is described by the Hamiltonian-

$$\begin{aligned} H &= \frac{1}{2m^*}[\mathbf{p} + e\mathbf{A}(x)]^2 + \frac{eg^*}{2m_0} \frac{\sigma\hbar}{2} B_z(x) \\ &= \frac{1}{2m^*}(p_x^2 + [p_y + eA(x)]^2) + \frac{eg^*}{2m_0} \frac{\sigma\hbar}{2} B_z(x) \end{aligned} \quad (1)$$

where  $m^*$  is the effective mass of the electron,  $\mathbf{p}$  is it's momentum,  $g^*$  the effective g-factor and  $m_0$  is the free-electron mass in vacuum,  $\sigma = +1/-1$  for up/down spin electrons, and  $\mathbf{A}(x)$ , the magnetic vector potential is given in the Landau gauge for the region  $-d/2 < x < d/2$  and for incoming electrons from the left by  $\mathbf{A}(x) = B_0\hat{y}$ , and for electrons incoming from the right by  $\mathbf{A}(x) = -B_0\hat{y}$ . The magnetic vector potential is zero otherwise. The last term in Eq. 1 is zero everywhere except at  $x = \pm d/2$ . For simplicity we introduce dimensionless units, the electron cyclotron frequency  $w_c = eB_0/m^*c$ , and the magnetic length  $l_B = \sqrt{\hbar c/eB_0}$ , with  $B_0$  being some typical magnetic field. All the quantities are expressed in dimensionless units: the magnetic field  $B_z(x) \rightarrow B_0 B_z(x)$ , the magnetic vector potential  $\mathbf{A}(\mathbf{x}) \rightarrow B_0 l_B \mathbf{A}(\mathbf{x})$ , the coordinate  $\mathbf{x} \rightarrow l_b \mathbf{x}$  and the energy  $E \rightarrow \hbar w_c E (= E_0 E)$ .

Since the Hamiltonian as depicted in Eq. 1 is translation-ally invariant along the  $y$ -direction, the total wave-function can be written as  $\Psi(x, y) = e^{iqy}\psi(x)$ , wherein  $q$  is the wave-vector component in the  $y$ -direction. Thus one obtains the effective one-dimensional Schroedinger equation-

$$\left[ \frac{d^2}{dx^2} - \{A(x) + q\}^2 - \frac{eg^*}{2m_0} \frac{\sigma m^*}{\hbar} B_z(x) + \frac{2m^*}{\hbar^2} E \right] \psi(x) = 0 \quad (2)$$

### III. THEORY

The S-matrix for electron transport across the device can be readily found out by matching the wave functions and as there are  $\delta$  function potentials there is a discontinuity in the first derivative. The wave functions on the left and right are given by  $\psi_1 = (e^{ik_1x} + r e^{-ik_1x})$  and  $\psi_3 = t e^{ik_1x}$ , while that in the region  $-d/2 < x < d/2$  is  $\psi_2 = (a e^{ik_2x} + b e^{-ik_2x})$ . The wave vectors are given by-  $k_1 = \sqrt{2E - q^2}$ ,  $k_2 = \sqrt{2E - (q + B_z)^2}$  and for electrons incident from the right,  $k_2$  in the wave-functions is replaced by  $k'_2 = \sqrt{2E - (q - B_z)^2}$ . Throughout this article, unless specified otherwise,  $q = 0$ , and therefore  $k'_2 = k_2$ .

With this procedure outlined above one can determine all the coefficients of the S-Matrix

$$S_\sigma = \begin{pmatrix} s_{\sigma 11} & s_{\sigma 12} \\ s_{\sigma 21} & s_{\sigma 22} \end{pmatrix} = \begin{pmatrix} r_\sigma & t'_\sigma \\ t_\sigma & r'_\sigma \end{pmatrix}$$

One can readily see from the transmission coefficients, for details see Ref.11 that there is no spin polarization as  $T_{+1} = T_{-1}$ . This fact was discovered only in Ref.12, two earlier works<sup>13,14</sup> had mistakenly attributed spin polarizability properties to the device depicted in FIG. 1. In the adiabatic regime, the device is in equilibrium, and for it to transport current one needs to simultaneously vary two system parameters  $X_1(t) = X_1 + \delta X_1 \sin(\omega t)$  and  $X_2(t) = X_2 + \delta X_2 \sin(\omega t + \phi)$ , in our case  $X_1$  is the width  $d$  and  $X_2$  the magnetic field  $B_z$  given in terms of the magnetization strength  $B_0 = M_0 h$ , where  $h$  is the height and  $M_0$  the magnetization of the ferro-magnetic stripe.

The pumped current can be calculated by using the procedure as adopted in Ref. 15 and in Ref. 16 for the case of a double barrier quantum well. A new formalism taking recourse to Floquet theory<sup>17</sup> has recently been applied to describe quantum pumping but in the following discussion we will concentrate only on Brouwer's approach as elucidated in Ref. 15. This approach has been further applied to several different systems, among them mention may be made of- quantum pumping in carbon nanotubes<sup>18</sup>, quantum pumping in systems with a super-conducting lead attached<sup>19</sup> and study of dephasing in quantum pumps<sup>20,21</sup>.

In the succeeding discussion, unless specified otherwise  $\alpha = 1$ , i.e., we always pump into the left lead or channel 1, (left of the barrier at  $-d/2$ , see Fig. 1(c)). The right lead or channel 2 is to the right of the barrier at  $d/2$ .

We further assume single moded transport in the leads or channels. Thus charge passing through lead  $\alpha$  due to infinitesimal change of system parameters is given by-

$$dQ_{\sigma\alpha}(t) = e\left[\frac{dN_{\sigma\alpha}}{dX_1}\delta X_1(t) + \frac{dN_{\sigma\alpha}}{dX_2}\delta X_2(t)\right] \quad (3)$$

with the current transported in one period being-

$$I_{\sigma\alpha} = \frac{ew}{2\pi} \int_0^\tau dt \left[ \frac{dN_{\sigma\alpha}}{dX_1} \frac{dX_1}{dt} + \frac{dN_{\sigma\alpha}}{dX_2} \frac{dX_2}{dt} \right] \quad (4)$$

In the above  $\tau = 2\pi/w$  is the cyclic period. The quantity  $dN_{\sigma\alpha}/dX_i$  is the emissivity which is determined from the elements of the scattering matrix, in the zero temperature limit by -

$$\frac{dN_{\sigma\alpha}}{dX_i} = \frac{1}{2\pi} \sum_{\beta} \Im\left(\frac{\partial s_{\sigma\alpha\beta}}{\partial X_i} s_{\sigma\alpha\beta}^*\right) \quad (5)$$

Here  $s_{\sigma\alpha\beta}$  denote the elements of the scattering matrix as denoted above, as evident  $\alpha, \beta$  and  $i$  can only take values 1,2, while  $\sigma$  takes values +1 or -1 depending on whether spin is up or down. The symbol “ $\Im$ ” represents the imaginary part of the complex quantity inside parenthesis.

The spin pump we consider is operated by changing the width and magnetic field strength  $B_z$  (given in terms of magnetization  $B_0 = M_0h$ ) of the ferro magnetic stripe, herein  $X_1 = d = d_0 + x_p \sin(\omega t)$  and  $X_2 = B_z = B_x + x_p \sin(\omega t + \phi)$ . A paragraph on the experimental feasibility of the proposed device is given above the conclusion. As the pumped current is directly proportional to  $w$  (the pumping frequency), we can set it to be equal to 1 without any loss of generality.

By using Stoke's theorem on a two dimensional plane, one can change the line integral of Eq. 4 into an area integral, see for details Ref.22-

$$I_{\sigma\alpha} = e \int_A dX_1 dX_2 \left[ \frac{\partial}{\partial X_1} \frac{dN_{\sigma\alpha}}{dX_2} - \frac{\partial}{\partial X_2} \frac{dN_{\sigma\alpha}}{dX_1} \right] \quad (6)$$

Substitution of Eq. 5 into Eq. 6 leads to,

$$I_{\sigma\alpha} = e \int_A dX_1 dX_2 \sum_{\beta=1,2} \Im\left(\frac{\partial s_{\sigma\alpha\beta}^*}{\partial X_1} \frac{\partial s_{\sigma\alpha\beta}}{\partial X_2}\right) \quad (7)$$

If the amplitude of oscillation is small, i.e., for sufficiently weak pumping ( $\delta X_i \ll X_i$ ), we have,

$$I_{\sigma\alpha} = \frac{ew\delta X_1 \delta X_2 \sin(\phi)}{2\pi} \sum_{\beta=1,2} \Im\left(\frac{\partial s_{\sigma\alpha\beta}^*}{\partial X_1} \frac{\partial s_{\sigma\alpha\beta}}{\partial X_2}\right) \quad (8)$$

In the considered case of a magnetic barrier the case of very weak pumping is defined by:  $x_p \ll B_x (= d_0)$ , and Eq. 8 becomes-

$$I_{\sigma\alpha} = I_0 \sum_{\beta=1,2} \Im\left(\frac{\partial s_{\sigma\alpha\beta}^*}{\partial B_z} \frac{\partial s_{\sigma\alpha\beta}}{\partial d}\right) \quad (9)$$

wherein,

$$I_0 = \frac{ewx_p^2 \sin(\phi)}{2\pi}$$

As we consider only the pumped currents into lead 1, therefore  $\alpha = 1$ . Further we drop the  $\alpha$  index in expressions below. From the elements of the S-Matrix given in Ref. 11, one can easily derive analytical expressions for the pumped current  $I_\sigma$ , pumped spin  $I_{sp}$  and charge  $I_{ch}$  currents in the very weak pumping limit addressed in Eq. 9, as follows-

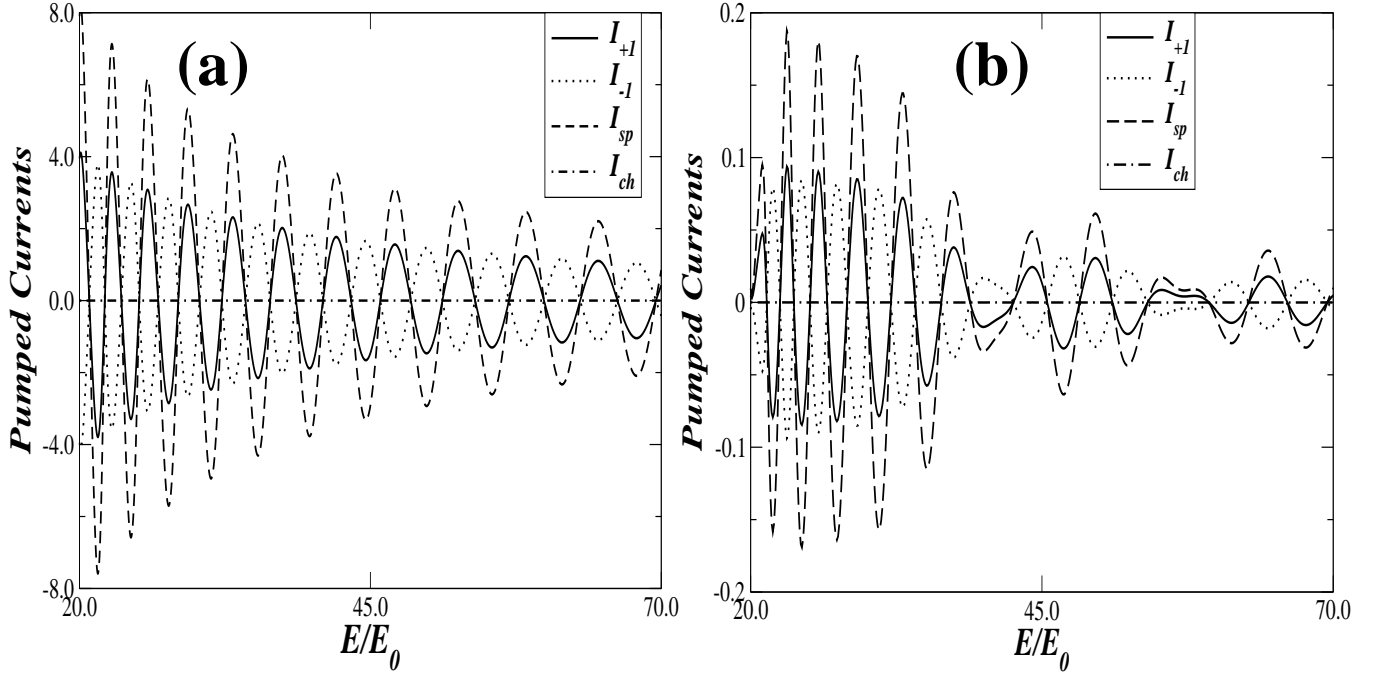


FIG. 2: Energy dependence of the pumped current. Spin polarized pumping delivering a net spin current along-with a vanishing charge current. The parameters are  $B_x = 5.0, d_0 = 5.0, \phi = \pi/2, g^* = 0.44$  and wave-vector  $q = 0$ . (a) The weak pumping regime. The pumped currents are normalized by  $I_0$ . In (b) the case of strong pumping for  $x_p = 1.0$  is plotted.

$$I_\sigma = \sigma I_0 \frac{2B_z^2 g^* g' k_1^3 k_2^2 \sin(2k_2 d)}{T_d^2}, \quad (10)$$

$$I_{sp} = I_{+1} - I_{-1} = I_0 \frac{4B_z^2 g^* g' k_1^3 k_2^2 \sin(2k_2 d)}{T_d^2}, \quad (11)$$

$$I_{ch} = I_{+1} + I_{-1} = 0, \quad (12)$$

$$\text{with } g' = 1 - \frac{g^{*2}}{4}, T_d = 4k_1^2 k_2^2 \cos^2(k_2 d) + [4E - g' B_z^2]^2 \sin^2(k_2 d),$$

and the wave-vectors are given by-

$$k_1 = \sqrt{2E} \text{ and } k_2 = \sqrt{2E - B_z^2}$$

It should be noted that the pumped charge current is identically zero, as the terms in the expression for  $I_{ch}$  cancel out resulting in zero pumped charge current in the weak pumping regime. In the succeeding sections we analyze the pumped spin and charge currents for different variations of parameters, in both the sufficiently weak pumping case (Eq. 9), as well as the general case of weak to strong pumping (Eq. 4).

#### IV. CHARACTERISTICS OF THE PUMPED CURRENT

In Fig. 2, we plot the pumped currents (magnified 100 times in Fig. 2(b)) as function of the Fermi energy at zero temperature for spin-up  $I_{+1}$  (solid-line), spin-down  $I_{-1}$  (dotted line), spin-polarized  $I_{sp} = I_{+1} - I_{-1}$  (dashed line) and the net charge current  $I_{ch} = I_{+1} + I_{-1}$  (dot-dashed line) in the special case of (a) very weak pumping (Eq. 9) and for the general case (Eq. 4) in (b). Again, unless specified otherwise, throughout the discussion temperature is always zero. The net charge current is expressed in terms of the electric charge. The parameters in dimensionless units are mentioned in the figure caption. The modulated parameters are out of phase by  $\pi/2$ . From Fig.2(a) and (b) it is evident that throughout the range of the Fermi-energy the net pumped charge current is negligible while a non-zero spin current is pumped. Quantitatively, for the general case of Fig.2(b) and for a *GaAs* based system,  $g^* = 0.44, m^* = 0.067m_e$  and if  $B_0 = 0.1\text{T}$  then  $l = 813\text{\AA}, \hbar\omega_c = E_0 = 0.17\text{mev}$ , thus for parameters in Fig. 2(b), energy  $E \sim 4.0 - 12.0\text{mev}$ ,

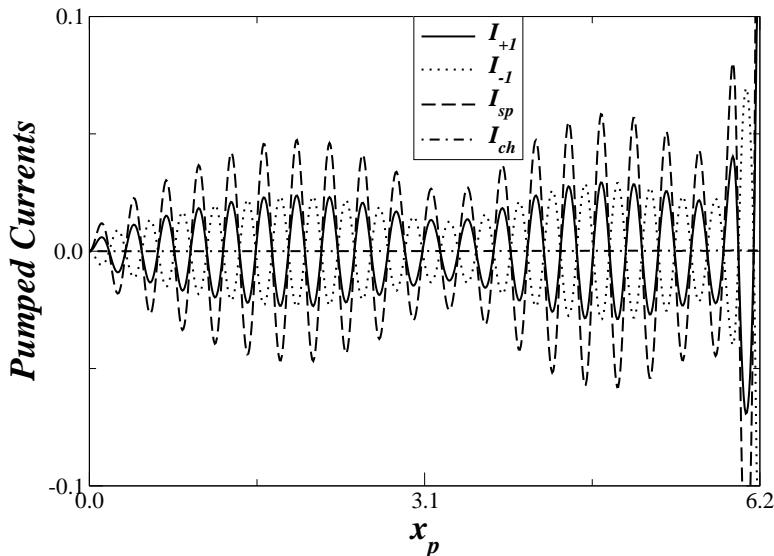


FIG. 3: Dependence of the pumped current on amplitude of pumping. Spin polarized pumping delivering a net spin current along-with a vanishing charge current. The parameters are  $d_0 = 5.0$ ,  $B_x = 5.0$ ,  $E/E_0 = 64.3$ ,  $\phi = \pi/2$ ,  $g^* = 0.44$  and wave-vector  $q = 0$ .

magnetic field strength  $B_x = 0.5\text{T}$ ,  $x_p=0.1\text{T}$ , and if  $w$  of the order of  $10^8$  Hz (as in the experimental arrangement of Switkes, et.al. in Ref. 3), then pumped spin current  $I_{sp} = 1.6 \times 10^{-19}\text{C} \times 10^8\text{Hz} \times 0.005 \sim 1 \times 10^{-13}\text{Amperes}$ , while the pumped charge current is  $10^4$  times weaker around  $10^{-17}\text{Amperes}$ . In Fig. 3 we plot the pumped spin and charge currents (from Eq. 4) as a function of  $x_p$ , the pumping amplitude for weak to strong pumping. We find a finite spin current with negligible charge current throughout the range of the pumping amplitude from the very weak to very strong. The figure 3, also conveys the very important fact that for the entire range, from the very weak to the very strong pumping regimes, we see increase in the magnitude of pumped currents which suggests that our model device would pump large spin currents in the very strong pumping regime. Further the pumped charge current is, for throughout the range of the pumping amplitude, zero. The physics behind the pumping mechanism in our model is as follows, in case of dc transport the transmittance is even in spin, as the Hamiltonian (Eq. 1) is time reversal invariant, as a consequence there is no spin polarization<sup>23</sup>, but herein as we consider the adiabatic modulation procedure, with the condition that the pumping amplitudes are out of phase by  $\phi$ , which implies the dynamical breaking of time reversal invariance which in turn leads to a net spin current being pumped. Recently it has been shown that for a ring with an oscillating scatterer (wherein potentials oscillate out of phase) the time reversal symmetry is dynamically broken and hence a net circulating (pumped) current arises<sup>24</sup>.

The pumped currents are sinusoidal as function of the phase difference for the weak pumping regime, but for the strong pumping regime this sinusoidal behavior is absent. In Fig. 4, we plot the pumped currents as a function of the phase difference  $\phi$  for Fermi energy  $E/E_0 = 23.12$ , for the case of weak pumping  $x_p = 0.1$  in (a), and the general case of strong pumping for  $x_p = 1.0$  in (b). In accordance with the results for a generic double barrier quantum pump, the pumped currents are anti-symmetric about  $\phi = \pi$  and maximum at  $\phi = \pi/2$  in (a), but in (b) we see that the relation between pumped currents and the phase difference is non-sinusoidal although they are still anti-symmetric about  $\phi = \pi$  and the currents peak at small difference in phase. In the strong pumping regime as it goes the magnitude of pumped currents are much larger than in the weak pumping regime, but in both the strong as well as weak pumping regimes the pumped currents are periodic with period  $2\pi$ . The figure 4 also conveys the important fact that throughout the range of the phase difference  $\phi$  we see zero pumped charge current, while the pumped spin currents are non-zero, and in figure 4(b) for the case of strong pumping the spin currents are much larger.

## V. IMPORTANCE OF RESONANCES

Resonances play an important role in the case of quantum pumping as exemplified in Refs.[16,25], in the following we depict the variation of the pumped currents with magnetic barrier strength and width of the magnetic barrier and show that this is indeed the case here also. In FIG. 5(a), we plot the pumped currents as a function of  $B_x$ , i.e., the

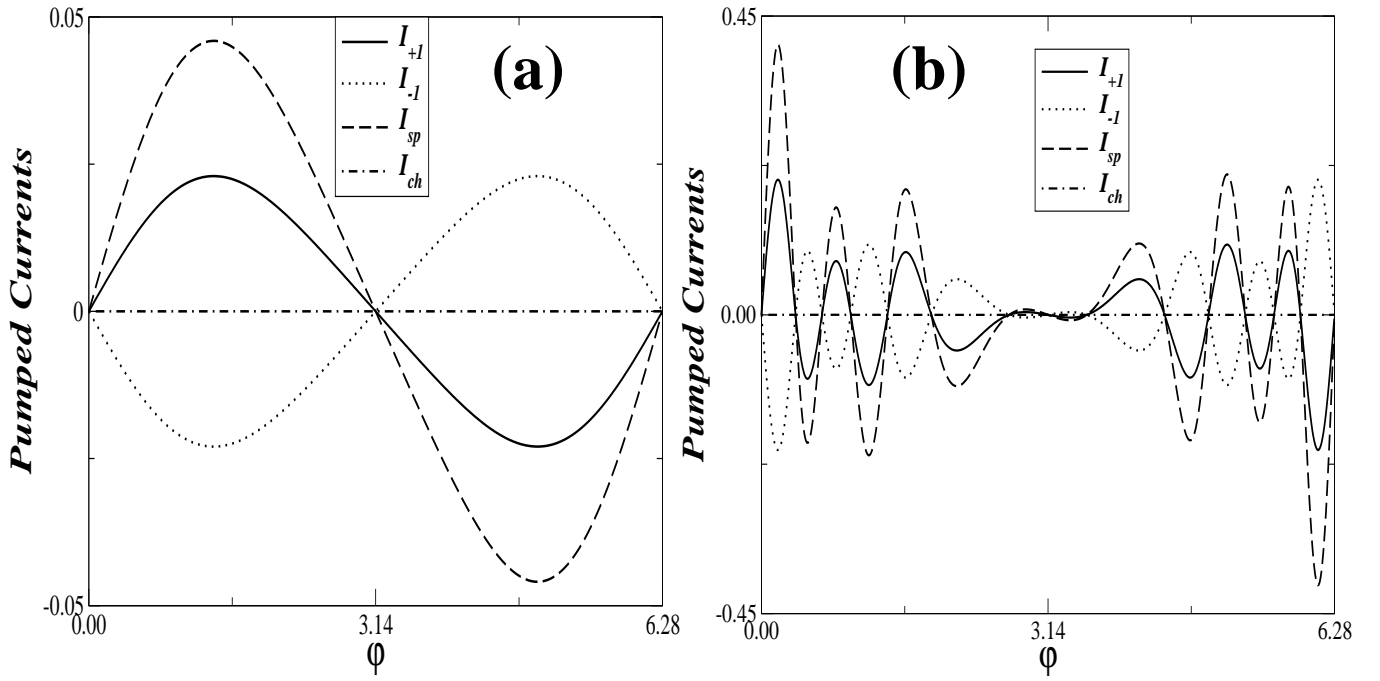


FIG. 4: Dependence of the pumped current on phase difference  $\phi$ . Spin polarized pumping delivering a net spin current along-with a vanishing charge current. (a) Weak pumping regime. The parameters are  $d_0 = B_x = 5.0$ ,  $x_p = .1$ ,  $E/E_0 = 23.12$  and wave-vector  $q = 0$ . (b) Strong pumping regime. The pumped currents are plotted for  $x_p = 1$  all other parameters remaining same.

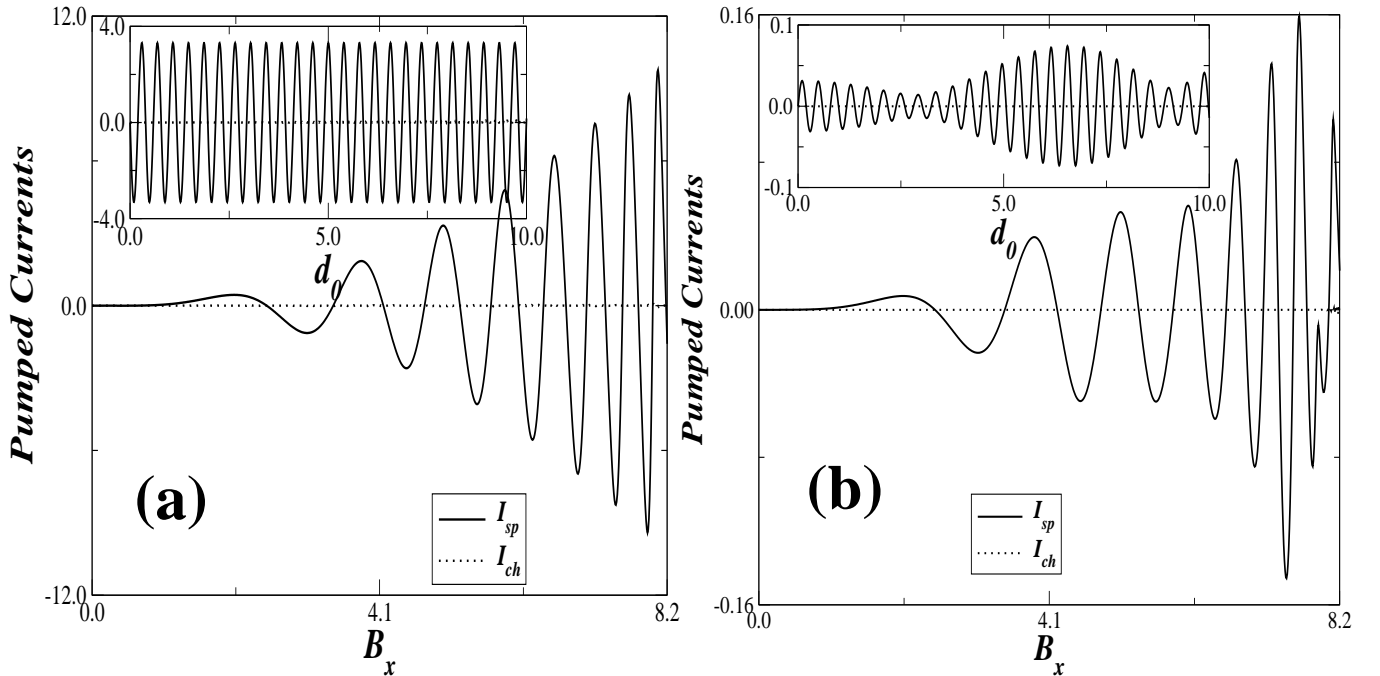


FIG. 5: Dependence of the pumped current on amplitude of barrier strength  $B_x$ . Spin polarized pumping delivering a net spin current along-with a vanishing charge current. (a) Weak pumping regime. The parameters are  $d_0 = 5.0$ ,  $\phi = \pi/2$ ,  $E/E_0 = 44.6$  and wave-vector  $q = 0$ . The pumped currents are normalized by  $I_0$ . (b) Strong Pumping regime  $x_p = 1.0$ . In the inset of (a) and (b) the pumped currents are plotted as function of the width  $d_0$ ,  $B_x = 5.0$ , all other parameters remaining same.

strength of the magnetic barrier, for Fermi energy  $E/E_0 = 44.6$  and phase difference  $\phi = \pi/2$  for the special case of very weak pumping as in Eq. 9 and in Fig.5(b) for the general case as in Eq. 4. The pumped currents depend on the strength of the barrier and for increased barrier strength these seem to be larger. As the Fermi energy is set at  $E/E_0 = 44.6$ , naturally a magnetic barrier of height of the order  $\sim 5.0$  or more will affect the electron and so naturally one sees increased pumping for larger values of  $B_x$ . In the inset of FIG. 5(a) and (b), we plot the pumped currents as a function of the  $d_0$ , i.e., the width of the magnetic barrier, for Fermi energy  $E/E_0 = 44.6$ . The pumped currents have almost a nice sinusoidal dependence on the width. Herein also as the resonances are controlled by the width one can explain these sinusoidal variations on the resonances of the system. From the analytical expression for the pumped currents (Eqs. 10-12) in the weak pumping regime one can easily notice that this sinusoidal dependence arises because of the  $\sin(2k_2d)$  factor in the numerator of Eqs.[10,11]. One can approximate  $g' \sim 1$  as  $g^* = 0.44$  for  $GaAs$  based system and thus the pumped current becomes-

$$I_\sigma \sim \sigma I_0 \frac{\sqrt{2E} B_z^2 g^* \sin(2k_2d)}{16E(2E - B_z^2) [1 + \frac{B_z^4}{8E(2E - B_z^2)} \sin^2(k_2d)]^2} \quad (13)$$

When  $2E \gg B_z^2$  one can neglect the second term inside the square bracket in the denominator of Eq. 13 as it is very small. Thus the pumped current in this limit reduces to

$$I_\sigma \sim \sigma I_0 \frac{B_z^2 g^* \sin(2k_2d)}{16E\sqrt{2E}}.$$

Thus we get the condition for resonances as  $2k_2d = (2n + 1)\pi/2, n = 0, 1, 2, \dots$ . The approximate position of the resonances in the  $2E \gg B_z^2$  regime, occur at Fermi energies-  $E_n = \frac{(2n+1)\pi}{8d} + \frac{B_z^2}{2}, n = 0, 1, 2, \dots$

## VI. SPIN-ORBIT SCATTERING

In the above analysis we have ignored the effects of spin-orbit scattering as this is generally supposed to be very small in these systems. However for a complete theory we have to include the effects of spin-orbit scattering, and

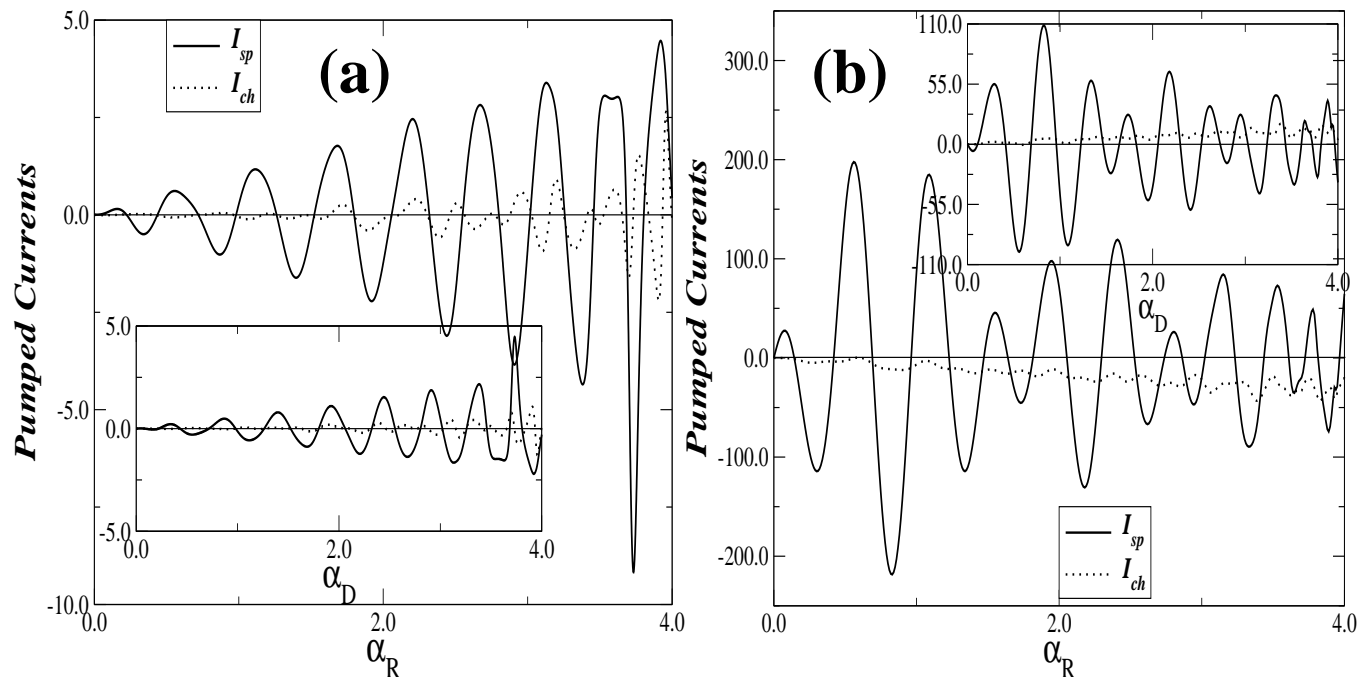


FIG. 6: Dependence of the pumped current on Rashba spin-orbit interaction  $\alpha_R$ . Spin polarized pumping delivering a net spin current along-with a small finite charge current. (a) Very weak pumping regime. The pumped currents are normalized by  $I_0$ . The parameters are  $B_x = 5.0, d_0 = 5.0, E/E_0 = 64.3, \phi = \pi/2$  and wave-vector  $q = 0$ . In the inset the dependence of the pumped currents on the Dresselhaus spin-orbit interaction  $\alpha_D$  is plotted, parameters remaining same. (b) Strong pumping case  $x_p = 1.0$  all other parameters remaining same. In the inset the dependence of the pumped currents on the Dresselhaus spin-orbit interaction  $\alpha_D$  is plotted, parameters remaining same.

analyze its impact on spin pumping. The spin-orbit scattering (SO) can arise due to two reasons<sup>26</sup>- (i) *Microscopic forces (Dresselhaus effect)*- In general III-V compounds (e.g., GaAs) lack inversion symmetry. This eventually leads to spin-orbit scattering induced splitting of the conduction band<sup>27</sup>. The magnitude of the splitting is proportional to cube of electron wave number  $k$ . In MOSFET's and hetero-structures, the host crystals are not treated as 3D systems, because crystal symmetry is broken at the interface where the 2DEG is dynamically confined in a quantum well. The reduction of effective dimensionality lowers symmetry of underlying crystals and results in an additional (linear in  $k$ ) term in the Dresselhaus splitting. It is seen that the linear in  $k$  term is dominant in GaAs quantum wells. (ii) *Macroscopic forces (Rashba effect)*- In addition to the above microscopic forces there is another source of splitting, an interface electric field<sup>28</sup>. It is manifest in a linear in  $k$  splitting of 2D band structure. In most 2DEG systems, the Rashba term dominates the Dresselhaus terms. Herein we first consider the Rashba spin-orbit interaction. In presence of this Rashba spin-orbit interaction the Hamiltonian defined in Eq. 1 is modified with the addition of the following term- $H_R = \alpha_R(\sigma_y p_x - \sigma_x p_y)$ . With this addition into the Hamiltonian only in region II (we assume the spin-orbit interaction only in the confines of the magnetic barrier), the wave-function is now described by two eigen-vectors corresponding to the Rashba split eigenvalues  $E_{1(2)} = E \pm \alpha_R \sqrt{2E + (q + B_z)^2}$ . Similar to the previous example one solves for the reflection and transmission amplitudes (see for details Ref.29) and calculates the pumped currents. Results are shown in Fig. 6(a) for the special case of very weak pumping (from Eq. 9) and in Fig. 6(b) for the general case (from Eq. 4). The inclusion of Rashba spin-orbit interaction leads to no change when  $\alpha_R$ , is small, i.e., the spin-orbit scattering length ( $l_{so} \sim \frac{1}{\alpha_R}$ ) is large. But increasing  $\alpha_R$  leads to a small charge current, which for  $l_{so} \ll d$  becomes significant, and of same order of magnitude as the spin current. Interestingly the spin-current oscillates as a function of  $\alpha_R$ , indicating the importance of interference effects. In the inset of Fig's. 6(a) and 6(b), we have depicted the effect of linear in  $k$  Dresselhaus type spin-orbit interaction,  $H_D = \alpha_D(\sigma_x p_x - \sigma_y p_y)$ . Similar to the Rashba type in this case also pumped currents behave correspondingly, as a function of the Dresselhaus spin-orbit interaction strength  $\alpha_D$ . It would also be worthwhile to point out that in-spite of the fact that a small charge current contribution manifests itself in the strong pumping regime, the magnitude of the pumped spin currents increases manifold both in case of Dresselhaus spin-orbit interaction and more so in case of Rashba spin-orbit interaction.

## VII. INELASTIC SCATTERING

Inelastic scattering has been ignored in our discussion so far, as we assume that the electron retains its phase coherence throughout the sample. This assumption has of-course limited validity as for low temperatures electron-phonon scattering is absent but electron-electron scattering is always present and may lead randomization of phase implying incoherent scattering and resulting in loss of coherence. To include inelastic (or incoherent) scattering so as to see its effect on the spin/charge ratio we follow the formalism developed in Ref.21. In this formalism a third fictitious voltage probe is coupled to the quantum pump and all inelastic processes culminating in dephasing are described by a single parameter  $\epsilon$ . In this model the Eq. 4, is modified to take into account inelastic processes in the

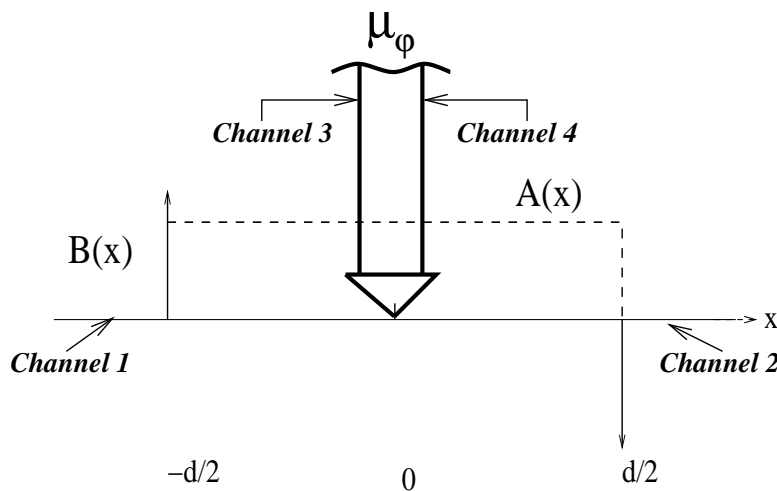


FIG. 7: The model magnetic field (delta function  $B(x)$ ) profile along with the magnetic vector potential  $A(x)$  in presence of a voltage probe  $\mu_\phi$  attached to inelastic channels 3 and 4.

following manner-

$$I_{\sigma 1} = \frac{ew}{2\pi} \int_0^\tau dt [F_{\sigma 1} + K_{in,\sigma 1}(F_{\sigma 3} + F_{\sigma 4})] \quad (14)$$

with the charge pumped given by

$$F_{\sigma\alpha} = \frac{dN_{\sigma\alpha}}{dX_1} \frac{dX_1}{dt} + \frac{dN_{\sigma\alpha}}{dX_2} \frac{dX_2}{dt},$$

and the emissivity is-

$$\frac{dN_{\sigma\alpha}}{dX_i} = \frac{1}{2\pi} \sum_{\beta} \Im \left( \frac{\partial s_{\sigma\alpha\beta}}{\partial X_i} s_{\sigma\alpha\beta}^* \right)$$

with  $\alpha = 1, 3, 4$  and the summation over  $\beta$  is for all channels 1, 2, 3, 4. The channels 3 and 4 are coupled to the voltage probe. The coefficient

$$K_{in,\sigma 1} = \frac{T_{\sigma,31} + T_{\sigma,41}}{T_{\sigma,31} + T_{\sigma,41} + T_{\sigma,32} + T_{\sigma,42}}$$

multiplied with the second term inside square brackets of Eq. 14, takes care of the re-injected electrons and hence current conservation.  $T_{\sigma ij}$ 's are the transmission coefficients from lead  $j$  to lead  $i$ . The above formula is for pumped current into lead (or, channel) 1 in presence of inelastic scattering and it is for the general case. For the special case of very weak pumping one can analogously as in section III, derive an expression for the pumped currents as follows-

$$I_{\sigma 1} = \frac{ewx_p^2 \sin(\phi)}{2\pi} [J_{\sigma 1} + K_{in,\sigma 1}(J_{\sigma 3} + J_{\sigma 4})] \quad (15)$$

where  $K_{in,\sigma 1}$  is as given above while  $J_{\sigma f}$ 's are given by-

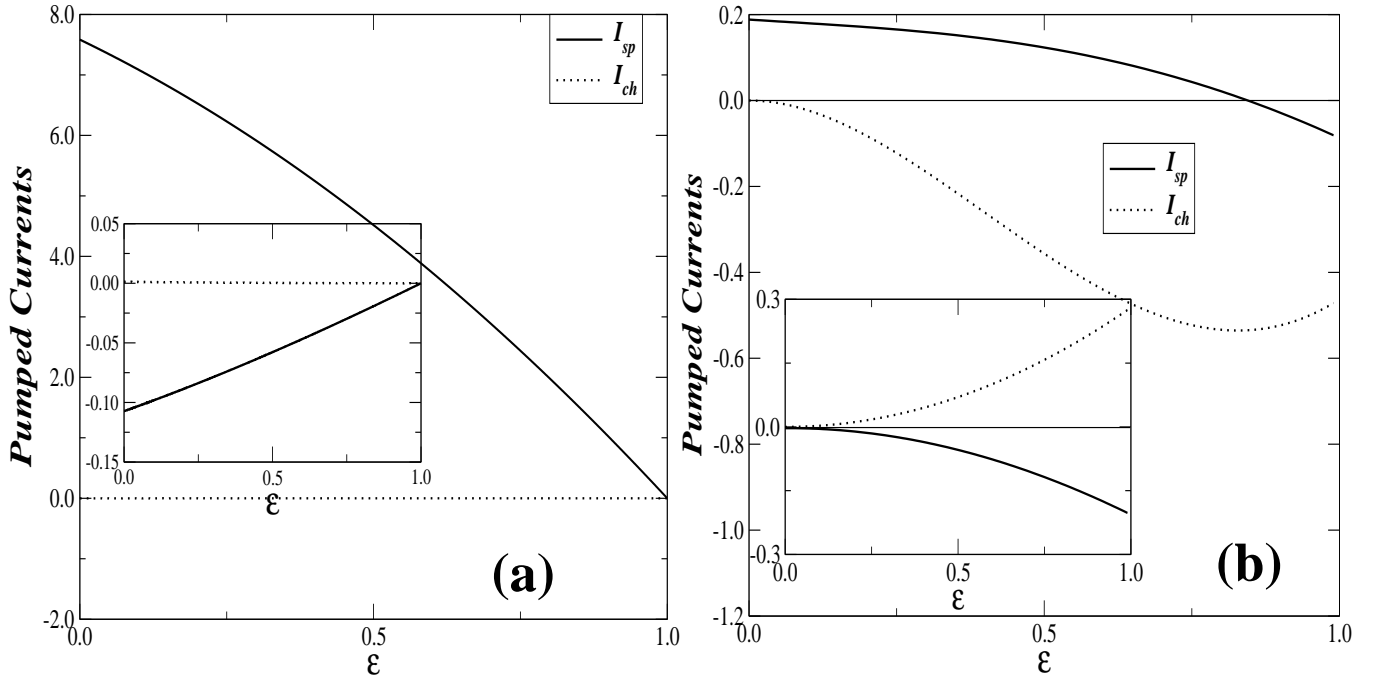


FIG. 8: Dependence of the pumped current on inelastic scattering  $\epsilon$ . Spin polarized pumping delivering a net spin current along-with a vanishing charge current in (a) Weak pumping regime. The pumped currents are normalized by  $I_0$ . The parameters are  $d_0 = 5.0$ ,  $B_x = 5.0$ ,  $\phi = \pi/2$ ,  $g^* = 0.44$ ,  $E/E_0 = 21.56$  and wave-vector  $q = 0$ . In the inset the pumped currents are plotted for non-resonant case  $E/E_0 = 22.17$  all other parameters remaining same. In (b) case of Strong pumping is considered. The parameters are  $d_0 = 5.0$ ,  $B_x = 5.0$ ,  $x_p = 1.0$ ,  $\phi = \pi/2$ ,  $g^* = 0.44$ ,  $E/E_0 = 23.0$  and wave-vector  $q = 0$ . In the inset the pumped currents are plotted for non-resonant case  $E/E_0 = 38.0$  all other parameters remaining same

$$J_{\sigma f} = \sum_{\beta} \Im \left( \frac{\partial s_{\sigma f \beta}^*}{\partial X_1} \frac{\partial s_{\sigma f \beta}}{\partial X_2} \right) \quad (16)$$

where the summation over  $\beta$  runs over all channels 1, 2, 3 and 4. An unique feature of including inelastic scattering in quantum pumps is that a new new physical mechanism of rectification comes into play in the fully incoherent limit. We consider the model system as in Fig. 7. The model system is coupled to a dephasing reservoir  $\mu_{\phi}$  via a wave-splitter located at  $x = 0$ . This wave-splitter is described by the S-Matrix-

$$S_{in} = \begin{pmatrix} 0 & \sqrt{1-\epsilon} & \sqrt{\epsilon} & 0 \\ \sqrt{1-\epsilon} & 0 & 0 & \sqrt{\epsilon} \\ \sqrt{\epsilon} & 0 & 0 & -\sqrt{1-\epsilon} \\ 0 & \sqrt{\epsilon} & -\sqrt{1-\epsilon} & 0 \end{pmatrix}$$

Here the coupling parameter  $\epsilon$  characterizes the strength of inelastic interactions. At  $\epsilon = 1$ , all electrons are inelastically scattered within the system, whereas at  $\epsilon = 0$ , the fictitious channels 3&4 are effectively decoupled from the system. In Fig.8(a) and (b), we plot the effect of inelastic interactions on both the pumped spin and charge currents for incident energy corresponding to a resonance in the system. In the special case of very weak pumping the charge current is essentially zero throughout, while spin-current decreases throughout till the maximum  $\epsilon = 1$  is reached but for strong pumping we see that the pumped charge current increases and in the  $\epsilon \rightarrow 1$  limit dominates the spin current. In the insets of (a) and (b) we plot the currents for non-resonant pumping, and herein the results in both cases do not differ much from the resonant case. With inelastic scattering the device still pumps spin current but now the pumped charge dominates but only in the strong pumping regime. In the weak pumping regime the pumped charge current is again zero throughout the range of the inelastic scattering parameter  $\epsilon$ . Of-course the model defined in Ref.21 and utilized earlier in analyzing inelastic effects in resonant tunneling diodes<sup>30</sup> assumes that an inelastic event takes place only at a particular point of the whole system. This is depicted in Fig. 7 by the triangle, the junction between the voltage probe and our model system. A more realistic model would be to couple the system to many such voltage probes at many points throughout the system. The relevant parameter in this model is then the probability that the electron be inelastically scattered while traversing the system. This parameter can be chosen to be  $\exp(-d/d_{\phi})$  as in Ref.31, wherein  $d$  is as defined above while  $d_{\phi}$  is the phase coherence length. This phase coherence length can be expressed in terms of the dephasing time ( $\tau_{\phi}$ ), as  $d_{\phi} = v_f \tau_{\phi}$  wherein  $v_f$  is the Fermi velocity of electrons traversing the system. Quantum mechanical coherence is lost on length scales larger than  $d_{\phi}$ . In the 4X4 S-Matrix defined above to take into account inelastic scattering, the inelastic scattering parameter  $\epsilon$  can be re-parametrized as  $1 - \exp(-d/d_{\phi})$ , to obviate this deficiency of single point inelastic scattering. For complete elastic scattering, i.e., in the limit  $d_{\phi} \gg d$ ,  $\epsilon \rightarrow 0$ , while for complete inelastic scattering,  $d_{\phi} \ll d$ ,  $\epsilon \rightarrow 1$ .

## VIII. NOISELESS TRANSPORT

The adiabatic quantum pump not only generates an electric current but also heat current which is the sum of the noise and power of joule heat. A quantum pump is termed optimal if it is noiseless<sup>32</sup>, i.e., if the total heat generated is only due to the joule heating. Following the procedure outlined in Refs.[33,34], one can derive an elementary formula for the heat current, joule heat and noise produced in the pumping mechanism.

The electric current generated in the pumping process and as in Eq. 4 can be reformulated as-

$$I_{\sigma\alpha} = \frac{ie}{2\pi\tau} \int_0^{\tau} dt \sum_{j=1,2} [\partial_{X_j} S_{\sigma} S_{\sigma}^{\dagger}]_{\alpha\alpha} \frac{\partial X_j}{\partial t} \quad (17)$$

The above formula is derived from the more general expression

$$I_{\sigma\alpha} = \frac{e}{\pi\tau} \int_0^{\tau} dt \int dE [S_{\sigma}(E, t) [f(E + i\partial_t/2) - f(E)] S_{\sigma}^{\dagger}(E, t)]_{\alpha\alpha} \quad (18)$$

One goes from Eq. 18 to Eq. 17 in the zero temperature limit and by expanding the Fermi Dirac distribution  $f(E + i\partial_t/2)$  up-to first order in  $\partial_t$ . See for details, Ref.[34]. One should also keep in mind the fact that by unitarity of the S-Matrix:  $-i(\partial_t S_{\sigma}^{\dagger} S_{\sigma})_{\alpha\alpha}$  equals  $\Im[\partial_t S_{\sigma}^{\dagger} S_{\sigma}]_{\alpha\alpha}$ . Here  $S_{\sigma}$  is the 2X2 S-Matrix as defined in section III. Again  $[\dots]_{\alpha\alpha}$  represents the  $\alpha\alpha^{th}$  element of the S-Matrix.

The heat current is defined as electric current multiplied by energy measured from the Fermi level-

$$H_{\sigma\alpha} = \frac{1}{\pi\tau} \int_0^\tau dt \int dE (E - E_F) [S_\sigma(E, t) [f(E + i\partial_t/2) - f(E)] S_\sigma^\dagger(E, t)]_{\alpha\alpha} \quad (19)$$

Expanding  $f(E + i\partial_t/2)$  up-to second order in  $\partial_t$ , one gets the heat current in the zero temperature limit as-

$$H_{\sigma\alpha} = \frac{1}{8\pi\tau} \int_0^\tau dt [\partial_t S_\sigma(E, t) \partial_t S_\sigma^\dagger(E, t)]_{\alpha\alpha} \quad (20)$$

Here the scattering matrix alluded to- “ $S_\sigma$ ”, is same as that in section III, with elements given in Ref.11. The heat current can be expressed as sum of joule heat and noise as follows-

$$\begin{aligned} H_{\sigma\alpha} &= \frac{1}{8\pi\tau} \int_0^\tau dt [\partial_t S_\sigma(E, t) \partial_t S_\sigma^\dagger(E, t)]_{\alpha\alpha} \\ &= \frac{1}{8\pi\tau} \int_0^\tau dt [\partial_t S_\sigma(E, t) S_\sigma^\dagger(E, t) S_\sigma(E, t) \partial_t S_\sigma^\dagger(E, t)]_{\alpha\alpha} \\ &= \frac{1}{8\pi\tau} \int_0^\tau dt \sum_{\beta=1,2} [\partial_t S_\sigma(E, t) S_\sigma^\dagger(E, t)]_{\alpha\beta} [S_\sigma(E, t) \partial_t S_\sigma^\dagger(E, t)]_{\beta\alpha} \end{aligned} \quad (21)$$

The diagonal term is identified as the joule heat while the off-diagonal term is the noise<sup>34</sup>. For  $\alpha = 1, \beta = 1, 2$ , the expression for the heat current can be shown to be broken into the noise and joule parts as follows-

$$\begin{aligned} H_{\sigma 1} &= J_{\sigma 1} + N_{\sigma 1} \\ &= \frac{1}{8\pi\tau} \int_0^\tau dt [\partial_t S_\sigma(E, t) S_\sigma^\dagger(E, t)]_{11} [S_\sigma(E, t) \partial_t S_\sigma^\dagger(E, t)]_{11} \\ &\quad + \frac{1}{8\pi\tau} \int_0^\tau dt [\partial_t S_\sigma(E, t) S_\sigma^\dagger(E, t)]_{12} [S_\sigma(E, t) \partial_t S_\sigma^\dagger(E, t)]_{21} \end{aligned} \quad (22)$$

When the pumping amplitude is very small one can similar to previous cases derive a formula for the heat current, joule heat produced and noise in our pumping mechanism as has been earlier derived for the heat current in Ref.33 and also for the noise in Refs.[35,36]. To derive the equations below we have taken  $\tau = 2\pi$ . Herein below we drop the ‘ $\alpha$ ’ index in the representation of the heat, joule and noise currents as it is assumed that we consider currents pumped into lead (or, channel) 1. Thus-

$$H_\sigma = \frac{w^2}{16\pi} [X_1^2 \sum_{\beta=1,2} |\frac{\partial s_{\sigma 1\beta}}{\partial X_1}|^2 + X_2^2 \sum_{\beta=1,2} |\frac{\partial s_{\sigma 1\beta}}{\partial X_2}|^2 + 2X_1 X_2 \cos(\phi) \sum_{\beta=1,2} \Re(\frac{\partial s_{\sigma 1\beta}}{\partial X_1} \frac{\partial s_{\sigma 1\beta}^*}{\partial X_2})] \quad (23)$$

$$\begin{aligned} J_\sigma &= \frac{w^2}{16\pi} [X_1^2 (\sum_{\beta=1,2} |s_{\sigma 1\beta}^* \frac{\partial s_{\sigma 1\beta}}{\partial X_1}|^2 + 2\Re(s_{\sigma 11} s_{\sigma 12}^* \frac{\partial s_{\sigma 11}^*}{\partial X_1} \frac{\partial s_{\sigma 12}}{\partial X_1})) + X_2^2 (\sum_{\beta=1,2} |s_{\sigma 1\beta} \frac{\partial s_{\sigma 1\beta}^*}{\partial X_2}|^2 + 2\Re(s_{\sigma 11} s_{\sigma 12}^* \frac{\partial s_{\sigma 11}^*}{\partial X_2} \frac{\partial s_{\sigma 12}}{\partial X_2})) \\ &\quad + 2X_1 X_2 \cos(\phi) (\sum_{\beta=1,2} |s_{\sigma 1\beta}|^2 \Re(\frac{\partial s_{\sigma 1\beta}}{\partial X_1} \frac{\partial s_{\sigma 1\beta}^*}{\partial X_2}) + \Re(s_{\sigma 11} s_{\sigma 12}^* \frac{\partial s_{\sigma 12}}{\partial X_1} \frac{\partial s_{\sigma 11}^*}{\partial X_2}) + \Re(s_{\sigma 12} s_{\sigma 11}^* \frac{\partial s_{\sigma 11}}{\partial X_1} \frac{\partial s_{\sigma 12}^*}{\partial X_2}))] \end{aligned} \quad (24)$$

$$\begin{aligned} N_\sigma &= \frac{w^2}{16\pi} [X_1^2 (\sum_{\beta=1,2} |s_{\sigma 2\beta}^* \frac{\partial s_{\sigma 1\beta}}{\partial X_1}|^2 + 2\Re(s_{\sigma 21} s_{\sigma 22}^* \frac{\partial s_{\sigma 11}^*}{\partial X_1} \frac{\partial s_{\sigma 12}}{\partial X_1})) + X_2^2 (\sum_{\beta=1,2} |s_{\sigma 2\beta} \frac{\partial s_{\sigma 1\beta}^*}{\partial X_2}|^2 + 2\Re(s_{\sigma 21} s_{\sigma 22}^* \frac{\partial s_{\sigma 11}^*}{\partial X_2} \frac{\partial s_{\sigma 12}}{\partial X_2})) \\ &\quad + 2X_1 X_2 \cos(\phi) (\sum_{\beta=1,2} |s_{\sigma 2\beta}|^2 \Re(\frac{\partial s_{\sigma 1\beta}}{\partial X_2} \frac{\partial s_{\sigma 1\beta}^*}{\partial X_1}) + \Re(s_{\sigma 21} s_{\sigma 22}^* \frac{\partial s_{\sigma 12}}{\partial X_2} \frac{\partial s_{\sigma 11}^*}{\partial X_1}) + \Re(s_{\sigma 22} s_{\sigma 21}^* \frac{\partial s_{\sigma 11}}{\partial X_2} \frac{\partial s_{\sigma 12}^*}{\partial X_1}))] \end{aligned} \quad (25)$$

In the above equations, ‘ $\Re$ ’ represents the real part of the complex quantity inside parenthesis. Since there are no correlations between electrons with different spin indices<sup>6</sup>, the noise of the charge current and of the spin current is simply  $N = N_{spin} = N_{charge} = N_{+1} + N_{-1}$ . Similarly the heat generated  $H = H_{spin} = H_{charge} = H_{+1} + H_{-1}$  and joule heat produced  $J = J_{spin} = J_{charge} = J_{+1} + J_{-1}$ . In Fig. 9, we plot the spin and charge currents along with

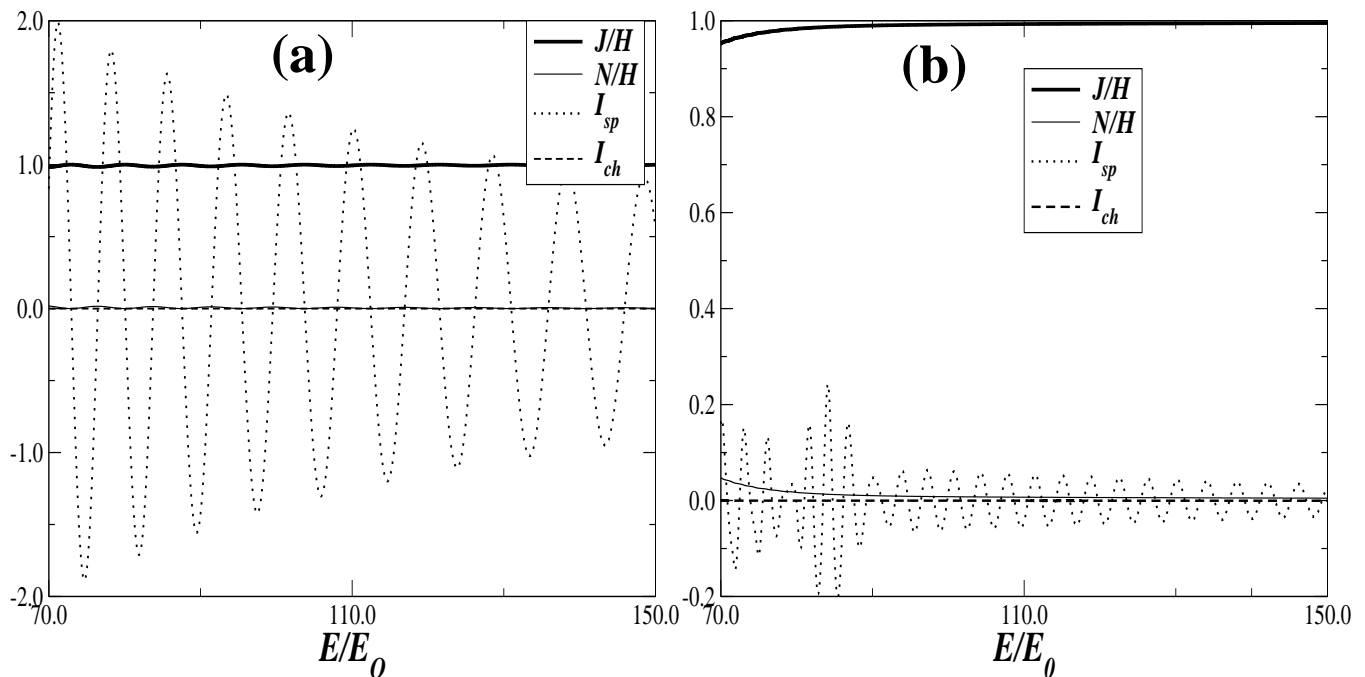


FIG. 9: Noise-less transport. (a) The weak pumping regime. Parameters are  $B_x = 5.0, d_0 = 5.0, \phi = \pi/2, q = 0.0$ , and  $g^* = 0.44$ . The pumped currents are normalized by  $I_0$ . (b) The strong pumping regime for  $x_p = 6.0, \phi = \pi/10$ , all other parameters remaining same.

the ratio of the power of joule heat to the heat current ( $J/H$ ) as also the ratio of the noise to heat current ( $N/H$ ) as function of the Fermi energy. We find that our pump is completely noiseless throughout the range of Fermi energies in the weak pumping regime. For very strong pumping in the initial range of Fermi energies ( $E/E_0 < 100.0$ ) the noise contribution to heat is small less than 4% while for  $E/E_0 > 100.0$  the noise is negligible less than 0.2% of the total heat generated. Almost all of the heat generated comes as a result of the joule power. Thus our model spin pump is almost optimal<sup>32</sup>. We have also checked that our spin pump remains optimal for a wide range of variation of parameters. In the case of weak pumping, the full counting statistics (distribution of the pumped charge/spin per cycle) is fully characterized by only two parameters<sup>37</sup>, the electric current generated  $I_\sigma$  (Eq. 9) and the noise  $N_\sigma$  (Eq. 25). The full counting statistics of our model quantum spin pump remains as an interesting problem and will be dealt with later on.

## IX. EXPERIMENTAL REALIZATION

To experimentally realize the above proposal, one can apply an external magnetic field to modulate the strength of magnetization of the Ferromagnetic stripe and this is one modulating factor, the other can be apart from the width of the stripe as has been employed in this work, the distance  $Z_0$  between stripe and 2DEG, which can be modulated by applying suitable gate voltages 'a la QPC', as has been done in the first experimental realization of the quantum pump<sup>3</sup>. Another method of experimentally realizing this proposal could be to put two such stripes side by side and applying different external magnetic fields to both, modulation of these external fields can effectively provide spin-polarized currents.

## X. CONCLUSIONS

To conclude, a spin polarized device acting on the principles of quantum adiabatic transport has been proposed. In the dc-transport case this device does not show any sign of spin-polarization as the system is time reversal invariant but in the adiabatic regime, when time reversal invariance is dynamically broken almost cent percent spin polarization is observed, incidentally in all the simulations, apart from the effects of inelastic scattering or to a lesser extent if significant spin-orbit scattering is present, we obtain zero charge current. As a welcome addition we see almost noiseless

transport i.e., realization of an optimal quantum spin pump. These features tell us that a adiabatically modulated magnetic barrier may be the best way to achieve not only quantum spin pumping but also optimal quantum spin pumping .

- 
- \* Electronic address: ronald@iopb.res.in  
† Electronic address: colin@iopb.res.in
- <sup>1</sup> D. J. Thouless, Phys. Rev. B **27**, 6083 (1983); F. Zhou, B. Spivak and B. Altshuler, Phys. Rev. Lett. **82**, 608 (1999).
  - <sup>2</sup> G. B. Lubkin, Physics Today June 1999, page 19; B. Altshuler and L I Glazman, Science **283**, 1864 (1999).
  - <sup>3</sup> M. Switkes, C. M. Marcus, K. Campman and A. C. Gossard, Science **283**, 1905 (1999); M. Switkes, Ph. D thesis, Stanford University (1999).
  - <sup>4</sup> P. W. Brouwer, Phys. Rev. B **63**, 121303 (2000).
  - <sup>5</sup> J. Wu, B. Wang, and J. Wang, Phys. Rev. B **66**, 205327 (2002); W. Zheng, et.al, Phys. Rev. B **68**, 113306 (2003); Y. Tserkovnyak, A. Brataas and G. E. W. Bauer, Phys. Rev. B **66**, 224403 (2002); P. Sharma and C. Chamon, Phys. Rev. Lett. **87**, 096401 (2001); T. Aono, Phys. Rev. B **67**, 155303 (2003).
  - <sup>6</sup> M. Governale, F. Taddei and R. Fazio, Phys. Rev. B **68**, 155324 (2003).
  - <sup>7</sup> S. K. Watson, R. M. Potok, C. M. Marcus and V. Umansky, cond-mat/0302492.
  - <sup>8</sup> E. R. Mucciolo, C. Chamon and C. M. Marcus, Phys. Rev. Lett. **89**, 146802, 2002.
  - <sup>9</sup> M. Lu, L. Zhang, Y. Jin and X. Yan, Eur. Phys. J. B **27**, 565 (2002).
  - <sup>10</sup> A. Matulis, F. M. Peeters and P. Vasilopoulos, Phys. Rev. Lett. **72**, 1518 (1994); F. M. Peeters and J. De Boeck in *Handbook of Nanostructured Materials and Nanotechnology*, edited by H. S. Nalwa, Volume 3, Electrical Properties (2000), Academic Press, page 345.
  - <sup>11</sup> The elements of the scattering matrix are given as follows:
$$r_{\sigma} = \frac{-i \sin(k_2 d)(k_1^2 - k_2^2 - \lambda^2 - 2i\lambda\sigma k_1)}{D}$$

$$t_{\sigma} = t'_{\sigma} = \frac{2k_1 k_2}{D}$$

$$r'_{\sigma} = \frac{-i \sin(k_2 d)(k_1^2 - k_2^2 - \lambda^2 + 2i\lambda\sigma k_1)}{D}$$
with  $D = 2k_1 k_2 \cos(k_2 d) - i \sin(k_2 d)(k_1^2 + k_2^2 + \lambda^2)$ ,  
 $\lambda = \frac{g^* B_z}{2}$ ,  $k_1 = \sqrt{2E}$  and  $k_2 = \sqrt{2E - B_z^2}$ .
- It should be noted here that the transmission amplitudes  $t_{\sigma}$  and  $t'_{\sigma}$  are spin-independent, spin-polarized pumping arises because of the spin-dependence of the reflection amplitudes.
- <sup>12</sup> G. Papp and F. M. Peeters, Appl. Phys. Lett. **79**, 3198 (2001).
  - <sup>13</sup> G. Papp and F. M. Peeters, Appl. Phys. Lett. **78**, 2184 (2001).
  - <sup>14</sup> A. Majumdar, Phys. Rev. B **54**, 11911 (1996).
  - <sup>15</sup> P. W. Brouwer, Phys. Rev. B **58**, R10135 (1998).
  - <sup>16</sup> Y. Wei, J. Wang and H. Guo, Phys. Rev. B **62**, 9947 (2000).
  - <sup>17</sup> M. Moskalets and M. Büttiker, Phys. Rev. B **66**, 205320 (2002); S. W. Kim, Phys. Rev. B **66**, 235304 (2002).
  - <sup>18</sup> Y. Wei, J. Wang, H. Guo and Christopher Roland, Phys. Rev. B **64**, 115321 (2001).
  - <sup>19</sup> M. Blaauboer, Phys. Rev. B **65**, 235318 (2002); J. Wang and B. Wang, Phys. Rev. B **65**, 153311 (2002).
  - <sup>20</sup> J. N. H. J. Cremers and P. W. Brouwer, Phys. Rev. B **65**, 115333 (2002).
  - <sup>21</sup> M. Moskalets and M. Büttiker, Phys. Rev. B **64**, 201305 (2001).
  - <sup>22</sup> Kai-An Cheng, An Adiabatic quantum electron pump, Final report for ENEE695, May 12, 2000.
  - <sup>23</sup> V. N. Dobrovolsky, D. I. Sheka and B. V. Chernyachuk, Surf. Sci. **397**, 333 (1998).
  - <sup>24</sup> M. Moskalets and M. Büttiker, Phys. Rev. B **68**, 075303 (2003).
  - <sup>25</sup> B. Wang, J. Wang and H. Guo, Phys. Rev. B **65**, 073306 (2002).
  - <sup>26</sup> A. V. Moroz and C. H. W. Barnes, Phys. Rev. B **60**, 14272 (1999).
  - <sup>27</sup> G. Dresselhaus, Phys. Rev. **100**, 580 (1955).
  - <sup>28</sup> Yu. A. Bychkov and E. I. Rashba, J. Phys. C: Solid State Physics **17**, 6039 (1984).
  - <sup>29</sup> Y. Jiang and M. B. A. Jalil, J. of Phys. Condensed Matter **15**, L31 (2003).
  - <sup>30</sup> M. Büttiker, Phys. Rev. B **33**, 3020 (1986); M. Büttiker, IBM J. Res. Dev. **32**, 63 (1988).
  - <sup>31</sup> H. F. Cheung, Y. Gefen and E. Riedel, IBM J. Res. Dev. **32**, 359 (1988).
  - <sup>32</sup> J.E. Avron, A. Elgart, G.M. Graf, and L. Sadun, Phys. Rev. Lett. **87**, 236601 (2000); J.E. Avron, A. Elgart, G.M. Graf, and L. Sadun, math-ph/0305049.
  - <sup>33</sup> B. Wang and J. Wang, Phys. Rev. B **66**, 125310 (2002).
  - <sup>34</sup> B. Wang and J. Wang, Phys. Rev. B **66**, 201305 (2002).
  - <sup>35</sup> M. Moskalets and M. Büttiker, Phys. Rev. B **66**, 035306 (2002).

<sup>36</sup> M. L. Polianski, M. G. Vavilov, and P. W. Brouwer, Phys. Rev. B **65**, 245314 (2002).

<sup>37</sup> L. S. Levitov, cond-mat/0103617.